

# Unusual Behavior of Antiferromagnetic Superconductors in Low Magnetic Fields

Krzysztof Rogacki

*Institut of Low temperature and Structure Research, Polish Academy of Sciences,  
50-950 Wroclaw, Poland*

---

## Abstract

In this article, we examine the superconducting properties of low- and high- $T_c$  magnetic superconductors in magnetic fields close to the first penetration field. Attention is paid to the properties that relate to the interactions between antiferromagnetism and superconductivity. It is suggested that several features characterizing the interplay between magnetic and superconducting subsystems in low- $T_c$  superconductors can also be present in high- $T_c$  materials, however, they have not been observed for any non-substituted antiferromagnetic superconductors of the Y123 type. For the  $\text{Gd}_{1+x}\text{Ba}_{2-x}\text{Cu}_3\text{O}_{7-\delta}$  compound, a peak in the temperature dependence of the ac susceptibility has been found for  $x = 0.2$  near the Néel temperature of the Gd sublattice. This peak is attributed to the suppression of superconducting persistent currents due to the pair breaking effect that results from the enhanced magnetic fluctuations in the vicinity of the phase transition temperature. This observation indicates that the interaction between magnetic and conducting electrons is present for the composition with  $x = 0.2$ , where magnetism is enhanced and superconductivity diminished.

*Key words:* Magnetic superconductors, First penetration field, Vortex dynamics, High- $T_c$  superconductors

*PACS:* 74.25.Ha, 74.60.Ec, 74.60.Ge, 74.70.Dd, 74.72.Jt

---

## 1 Introduction

Magnetism and superconductivity are two forms of long-range order that may exist in a material at appropriate low temperatures. When both are present and the singlet state pairing occurs, they compete with one another, and many

---

*Email address:* [rogacki@int.pan.wroc.pl](mailto:rogacki@int.pan.wroc.pl) (Krzysztof Rogacki).

authors have wondered under what conditions they might coexist. The answer has been emerging in recent years, but the story began many years ago with theoretical works by Ginzburg [1], Abrikosov and Gorkov [2], and experimental studies by Matthias and co-workers that intensively examined the solid solutions  $\text{La}_{1-x}\text{RE}_x$  [3] and  $\text{RERu}_2$  [3,4] (RE = magnetic rare earth ions). In  $\text{La}_{1-x}\text{RE}_x$ , superconductivity was destroyed by relatively small amounts of paramagnetic ions ( $\simeq 1$  at.%), well before the long-range magnetic order appeared. These experiments showed that superconductivity was suppressed by the so-called  $s$ - $f$  exchange interaction between conduction electrons and localized  $f$ -shell spins [3,5].

After many years of extensive studies of alloys and disordered compounds with paramagnetic impurities it became clear that long-range magnetic order and singlet state superconductivity may coexist only in weak limit of the  $s$ - $f$  exchange interaction [6]. One of the simplest ways to fulfil this requirement consists in the spatial separation of conduction and magnetic electrons. This idea was first realized along with the discovery of ternary compounds like  $\text{RERh}_4\text{B}_4$  and the  $\text{REMo}_6\text{S}_8$  Chevrel phases [7]. Most of these compounds become superconducting below a temperature  $T_c$  despite the presence of a relatively large amount of the rare earth magnetic ions ( $\simeq 11$  at.% for  $\text{RERh}_4\text{B}_4$ ). Moreover, many of them show long-range magnetic order in the superconducting state. For ferromagnetic (FM) order, superconductivity can be preserved only in a very narrow temperature range, just below the Curie temperature. However, when the magnetic order is antiferromagnetic (AFM), superconductivity remains below the Neel temperature,  $T_N$ , down to the lowest investigated temperatures. The main reason for the observed coexistence of superconductivity and long-range antiferromagnetism seems to be the particularly weak exchange interaction due to the partial separation of the conduction  $4d$  electrons in  $k$ -space from the localized  $4f$  electrons of the rare earth ions due to the cluster structure of these compounds.

In layered low- $T_c$   $\text{RENi}_2\text{B}_2\text{C}$  superconductors [8,9,10,11], the spatial separation between conduction electrons, mostly Ni 3d [12], and magnetic electrons, RE 4f, is no longer clear. However, the weakness of the exchange interaction and, therefore, the presence of coexistence may still be understood. In these compounds, where RE = Dy, Ho, Er, and Tm, the hybridization of  $4f$  and conduction electrons is weak and a partial separation between those electrons appears in momentum space. For RE = Pr, Nd, Pm, Sm, Eu, Gd, and Tb, the absence of superconductivity involves several reasons which are beyond the scope of this article and are reviewed elsewhere [13].

In the case of layered high- $T_c$   $\text{REBa}_2\text{Cu}_3\text{O}_7$  (RE123) superconductors, the coexistence between long-range antiferromagnetism and superconductivity seems to be more puzzling. In these compounds the magnetic RE ions are located between the double  $\text{CuO}_2$  planes that are responsible for superconductivity.

Here, as for the layered low- $T_c$  superconductors, the long-range AFM order of the RE ions is realized via the RKKY and/or superexchange interactions [14]. For the RE123 materials, however, a modified exchange mechanism is necessary because the RE magnetic moments and the conduction electrons interact very weakly [15,16]. An additional reason that the coexistence of AFM order and superconductivity occurs in high- $T_c$  superconductors may be the extremely short coherence length,  $\xi$ , about 15 Å in the ab-plane.

For low- $T_c$  classic and layered magnetic superconductors, the unusual behavior of the upper critical field near and below  $T_N$  has been widely explored to verify pair-breaking interactions that arise when magnetic and superconducting subsystems coexist [17,18,19,20]. For high- $T_c$  superconductors, the upper critical fields at temperatures where the magnetic order appears are generally unavailable in the laboratory [21,22,23]. In this work, we discuss some low field effects that allow us to study the interaction between antiferromagnetism and superconductivity in high- $T_c$  materials.

## 2 Unusual vortex dynamics in clastic antiferromagnetic superconductors

The temperature dependence of the lower critical field,  $H_{c1}(T)$ , was studied close to  $T_N$  in GdMo<sub>6</sub>Se<sub>8</sub> [24]. The obtained results show the vortex dynamics of isolated vortex lines during the flux first penetration process. The most striking feature of the  $H_{c1}(T)$  curve is a drastic dip of  $H_{c1}$  observed at  $T_N$ . This irregularity is a simple consequence of the pair-braking effect caused by fluctuations enhanced near a phase transition. Similar unusual behavior of  $H_{c1}(T)$  is expected for high- $T_c$  antiferromagnetic superconductors in the case when the conduction and magnetic electrons interact.

Flux penetration was considered in detail for classic magnetic superconductors when the magnetic subsystem is a two-sublattice antiferromagnet with the easy axis oriented parallel to the external field [25,26]. Fig. 1 shows the phase diagram of the two-sublattice antiferromagnet, where the antiferromagnetic (AFM), spin-flop (SF), and paramagnetic (PM) phases are present depending on the magnetic field and temperature. This property requires the vortex line to have a special magnetic structure when the field in the vortex core is larger than the SF transition field,  $H_{SF}$ . When the density of vortices increases, the spin-flop phase enlarges and the individual vortex may have a magnetic structure as presented in Fig. 2. Consider the flux penetration process into the AFM superconductor in the case when the vortices with the described structure appear for  $H$  close to  $H_{c1}$ . It has been predicted that such vortices have a new surface barrier for penetration [26]. Thus, the flux penetration process proceeds in two steps, as shown in Fig. 3. With increasing  $H$  (see

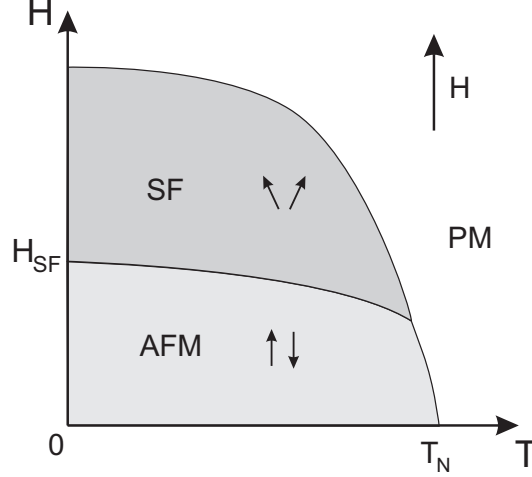


Fig. 1. Phase diagram of the two-sublattice antiferromagnet with the easy axis oriented parallel to the external field direction.  $H_{SF}$  is the field at which the transition from the antiferromagnetic (AFM) to the spin-flop (SF) phase occurs.

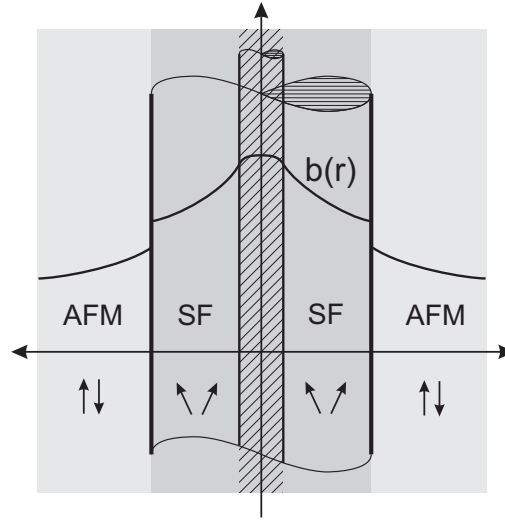


Fig. 2. Magnetic structure of the isolated vortex and the distribution of magnetic induction ( $b(r)$ ) around the vortex core in the spin-flop (SF) and antiferromagnetic (AFM) phases [25,28]. Dashed area illustrates the vortex core.

Fig. 3a), the Meissner effect ( $B = 0$ ) is observed until  $H$  reaches the value of the first penetration field,  $H_{en1}$ . Then, the usual flux penetration process begins and  $B$  increases. Next, when the field in the vortex core is higher than  $H_{SF}$ , the SF phase appears and the new shielding ( $B = \text{const}$ ) should be observed. For  $H$  increased above the characteristic value  $H_{en2}$  (the second penetration field), the magnetic flux penetrates the superconductor again. The  $B(H)$  dependence can be transformed to the  $M(H)$  dependence which can be easily measured at constant temperature. Fig. 3b shows the  $M(H)$  virgin curve for the two-step flux penetration process expected for an AFM superconductor magnetized in  $H$  oriented parallel to the magnetic easy axis.

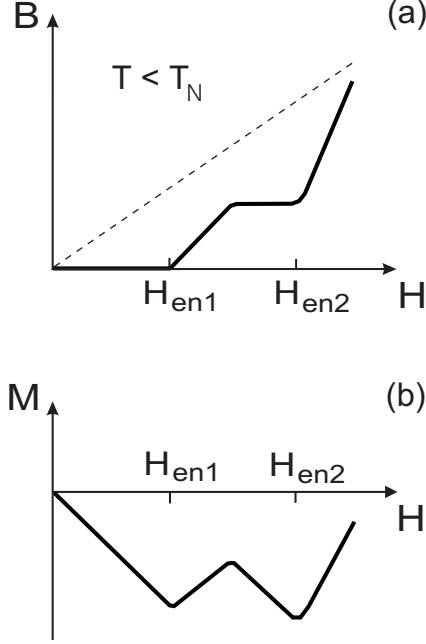


Fig. 3. Two-step flux penetration expected for the virgin magnetization process of an antiferromagnetic superconductor. The  $B(H)$  dependence (a) is transformed to the  $M(H)$  dependence (b). The magnetic easy axis of the superconductor is parallel to the external field direction.

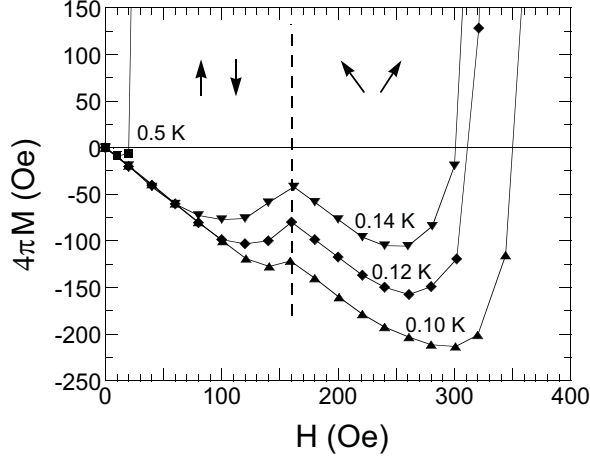


Fig. 4. Magnetization as a function of applied field for the virgin state of the  $\text{DyMo}_6\text{S}_8$  single crystal with the magnetic easy axis parallel to the field direction. As predicted, two-step flux penetration is observed below  $T_N = 0.4$  K. The arrows show the possible configuration of the spin of Dy ions in the vortex core. [27]

The single crystal of  $\text{DyMo}_6\text{S}_8$  was studied by magnetization measurements below and above  $T_N = 0.40$  K [27]. The single crystal was a cube with the edge dimension of 0.2 mm and a mass  $m \simeq 0.05$  mg. It was oriented with the magnetic easy axis (the [111] crystallographic triple axis) parallel to the applied magnetic field,  $H$ . For that orientation, the demagnetizing factor was assumed to be  $k = 1/3$ . Fig. 4 shows the unusual flux dynamics caused by the

appearance of the SF phase in the superconducting state. Here, magnetization behaves in the way as predicted and illustrated in Fig. 3b. Two-step flux penetration is clearly observed at  $T < T_N$  and  $H_{en2}(0.1 \text{ K}) \simeq 310 \text{ Oe}$  is found after correction for demagnetizing effects.

The two-step flux penetration can be analyzed in the framework of phenomenological theory with the free energy of an AFM superconductor expressed in the following form [28]:

$$F = \int dv \left\{ f_S + f_M + \frac{1}{8\pi} (\mathbf{b} - 4\pi\mathbf{M})^2 \right\}, \quad (1)$$

where  $\mathbf{b}$  is the microscopic magnetic induction and  $\mathbf{M} = \mathbf{M}_1 + \mathbf{M}_2$  is the magnetization of a two-sublattice antiferromagnet. The superconducting component is introduced in the Ginzburg-Landau (GL) form:

$$f_S = \frac{\hbar^2}{2m} \left| \left( \nabla - \frac{2ie}{c\hbar} \mathbf{a} \right) \Psi \right|^2 + \alpha |\Psi|^2 + \frac{1}{2} \beta |\Psi|^4, \quad (2)$$

where  $e$  and  $m$  denote the charge and mass of an electron, respectively,  $c$  is the velocity of light,  $\mathbf{a}$  is the vector potential,  $\Psi$  is the superconducting order parameter, and  $\alpha$  and  $\beta$  are some phenomenological expansion coefficients. The AFM energy is given by the following expression:

$$f_M = J\mathbf{M}_1 \cdot \mathbf{M}_2 + K \sum_{i=1}^2 (M_i^z)^2 - |\gamma| \sum_{i=1}^2 \sum_{j=x,y,z} (\nabla M_i^j)^2, \quad (3)$$

where  $J$  is the exchange constant between two AFM sublattices,  $K$  denotes the single ion anisotropy constant, and  $\sqrt{|\gamma|}$  is the magnetic stiffness length. According to experiments, the so-called  $s$ - $f$  exchange interaction is weak [18]. This means that superconductivity ( $\Psi$ ) and magnetism ( $\mathbf{M}$ ) interact via the electromagnetic interaction and the order parameters are coupled via the vector potential  $\mathbf{a}$ :

$$\begin{aligned} \mathbf{b} &= \nabla \times \mathbf{a}, \\ \mathbf{j}_s(\Psi^+, \Psi) &= \frac{c}{4\pi} \nabla \times (\mathbf{b} - 4\pi\mathbf{M}). \end{aligned} \quad (4)$$

The equilibrium conditions of the whole system can now be obtained by minimization of the Gibbs free energy functional,

$$G = F - \frac{1}{4\pi} \int \mathbf{b} \cdot (\mathbf{b} - 4\pi\mathbf{M}) dv, \quad (5)$$

with respect to  $\Psi$ ,  $\mathbf{a}$ , and  $\mathbf{M}$ . Then, an expression for  $H_{en2}(B)$  is obtained as a final result [28]

$$H_{en2}(B) = \sqrt{B^2 + H_{en2}^2(0)}, \quad (6)$$

where:

$$2H_{en2}(0) = \frac{H_{SF}}{\sqrt{\frac{\varphi_0}{\pi\lambda^2 B_{SF}} \ln\left(\frac{\pi\lambda^2 B_{SF}}{\varphi_0}\right)}},$$

$$H_{SF} = 2H_{c1} + z \frac{\varphi_0}{2\pi\lambda^2} K_0\left(\frac{d}{\lambda}\right). \quad (7)$$

Here,  $\varphi_0$  is a flux quantum,  $\lambda$  is a penetration depth,  $z$  is a coordination number,  $K_0$  is the modified Bessel function, and  $d$  is a distance between the nearest vortices.  $H_{SF}$  is a thermodynamic critical field at which the transition to the SF phase appears.

The experimental and calculated results obtained for DyMo<sub>6</sub>S<sub>8</sub> are shown in Table 1. They agree well and this seems to support the assumption that the dominant interaction between superconducting and magnetic subsystems is the electromagnetic one, even at low magnetic fields. This assumption is sufficient to describe quantitatively the anomalous virgin magnetization curves observed in the AFM superconducting state.

Table 1

The experimental (exp) and calculated (cal) second penetration field,  $H_{en2}$ . The experimental values were obtained from Fig. 4 after correction for demagnetizing effects.

$T$ [K]	$H_{en2}(\text{exp})$ [Oe]	$H_{en2}(\text{cal})$ [Oe]
0.14	260	215
0.12	290	240
0.10	310	265

The two-step flux penetration process was used to estimate the number of magnetic ions in the vortex core, and then,  $\xi$  and  $\kappa$  (the GL parameter) in the AFM superconducting state [27]. The significant reduction of  $\lambda$  was observed leading to a strong compression of the quantized flux and resulting in a considerable decrease of  $\kappa$  from 11, obtained for  $T$  just above  $T_N$ , to about 2.5 for  $T$  below  $T_N$ . The large reduction of  $\kappa$  provides evidence that on decreasing temperature the AFM superconductor tends to transform from a type-II to a type-I superconductor, as predicted theoretically in [29,30] and

confirmed experimentally for the ferromagnetic superconductor  $\text{ErRh}_4\text{B}_4$  [31]

### 3 Interaction between antiferromagnetism and superconductivity in selected high- $T_c$ materials

Polycrystalline Gd123 was chosen to obtain  $H_{c1}$  as a function of  $T$  close to  $T_N = 2.2$  K to investigate the possible interaction between the antiferromagnetic and superconducting subsystems [32]. Monotonic dependence of  $H_{c1}(T)$  was observed and interpreted as evidence that no pair breaking is present and that the AFM subsystem is effectively screened by superconductivity. This has been confirmed by ac susceptibility,  $\chi_{ac}$ , measured as a function of  $T$  with an ac field  $h_{ac} \leq 10$  Oe at 200 Hz that has not revealed any AFM peak at  $T_N$ .

The two-step flux penetration in layered high- $T_c$  superconductors was considered in detail theoretically in [33]. Two cases were examined. In the first, the external field was applied parallel to both the  $\text{CuO}_2$  layers and the magnetic easy axis. In the second, the external field was parallel to the layers but perpendicular to the easy axis. The calculations showed that in the first case the vortex line has a complex magnetic structure for  $H_{en1} < \frac{1}{2}H_{SF}$  and the external field exceeds the value  $\frac{1}{2}H_{SF}$ . This structure consists of a SF domain which is first created along the vortex core, like in classic magnetic superconductors (see Fig. 2). The appearance of this structure may have a profound effect on both classic and quantum flux creep in AFM high- $T_c$  superconductors [34].

Dy123 single crystals with  $T_c = 88$  K and  $T_N = 0.9$  K were used to verify the two-step flux penetration process in magnetic high- $T_c$  superconductors [35]. Magnetization virgin curves  $M(H)$  were studied with a vibrating reed technique at  $T < T_N$  and  $H$  parallel to the  $c$ -axis. For fully oxygenated Dy123, the  $c$ -axis is parallel to the magnetic easy axis [36,37], thus the sample-field orientation fulfills the requirement to observe two-step flux penetration [33]. No anomalous behavior of  $M$  was found for the field value for which the transition from the AFM to the SF phase occurs.  $M(H)$  curves follow the analytical result for a type-II superconducting stripe in a perpendicular magnetic field. This suggests a weak interaction between superconducting and localized magnetic electrons and provides verification that the existing reorientation in the magnetic subsystem is externally shielded and can not be observed by magnetic or transport measurements. In that case, the possible interaction between antiferromagnetism and superconductivity may be expected to be revealed when antiferromagnetism is enhanced and/or superconductivity diminished. There are several ways to lower  $T_c$  in the Y123 type superconductors. One way is to reduce the oxygen content much below 7 in a stoichiometric compound [38,39,40]. Another is substitution of RE for Ba [41,42,43,44] or Sr

for Ba [45,46,47]. Yet another uses a weak Josephson coupling between grains in ultrathin Dy123 films [48]. For these films, a clear peak was observed at  $T_N$  for resistance measured as a function of temperature. The peak was interpreted as a result of the reduction of the intergranular Josephson coupling by pair breaking due to enhanced intragranular spin-disorder scattering at  $T_N$ .

Samples of  $\text{Gd}_{1+x}\text{Ba}_{2-x}\text{Cu}_3\text{O}_{7-\delta}$  solid solution were synthesized resulting in superconductors with  $T_c$  decreasing from 93 K to about 40 K and  $T_N$  increasing from 2.24 to 2.45 K for  $x$  changing from 0 to 0.2. The final heat treatment was performed for 24 hours at 400 °C in oxygen and 700 °C in Ar to obtain superconducting and non-superconducting samples, respectively. For the superconducting samples, the maximized oxygen content increased from 6.93 to 7.03 for substitution levels varying from  $x = 0$  to  $x = 0.2$ . Details about the preparation procedure were published elsewhere [49]. Fig. 5 shows  $T_c(x)$  and  $T_N(x)$  dependencies that reveal the composition with  $x = 0.2$  as optimal for our purpose. For samples with  $x > 0.2$ ,  $T_N$  decreases and the peak observed in specific heat measurements at  $T_N$  gets smaller and wider indicating that the Gd ions may not be perfectly magnetically ordered and, quite probably, they are also not homogeneously distributed.

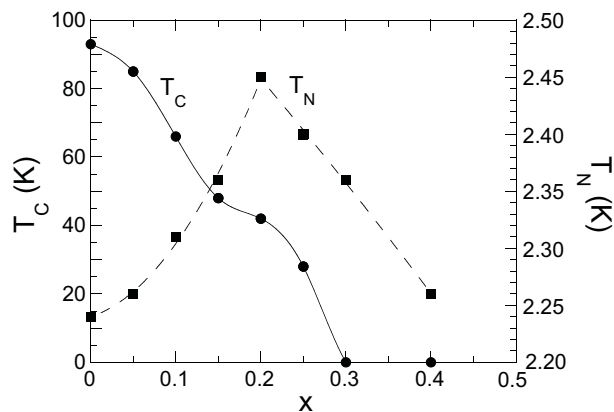


Fig. 5. Superconducting transition temperature,  $T_c$ , and antiferromagnetic order temperature,  $T_N$ , versus composition  $x$  for oxygen annealed  $\text{Gd}_{1+x}\text{Ba}_{2-x}\text{Cu}_3\text{O}_{7-\delta}$ .

Fig. 6 shows the  $\chi_{ac}'(T)$  results obtained for the oxygen annealed samples with  $x = 0.05$  (Fig. 6a) and 0.2 (Fig. 6b). A pronounced peak at  $T_N$  is observed at  $H = 6$  kOe for the  $x = 0.2$  sample. This peak is interpreted as evidence that the magnetic and superconducting subsystems interact and superconductivity is not able to screen the AFM fluctuations being enhanced close to the phase transition. We believe that the pair breaking effect is a simple reason for the observed peak. This effect can not be studied in the usual way because  $H_{c2}$  is still too high to be measured at temperatures close to  $T_N$  for the sample with  $x = 0.2$ .

Fig. 7 shows the low temperature part of  $\chi_{ac}'(T)$  obtained for the oxygen

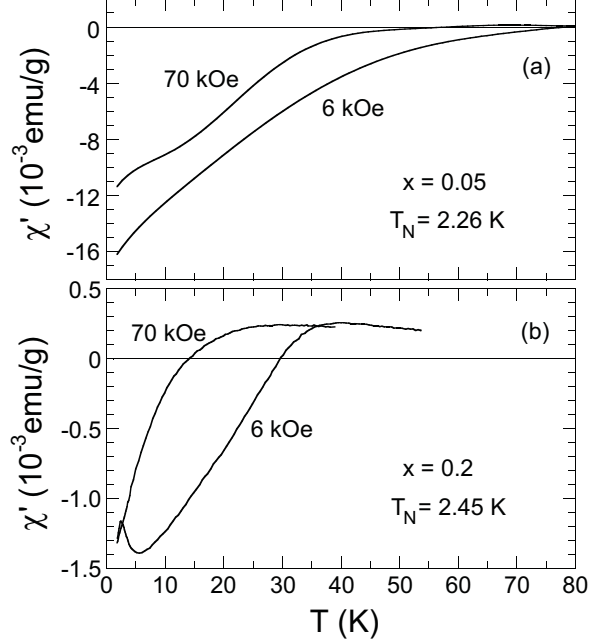


Fig. 6. Real part of the ac susceptibility,  $\chi'$ , for the oxygen annealed  $\text{Gd}_{1+x}\text{Ba}_{2-x}\text{Cu}_3\text{O}_{7-\delta}$  samples with  $x = 0.05$  (a) and  $0.2$  (b) measured at  $H = 6$  and  $70$  kOe. Clear anomaly is present at  $T_N$  for the  $x = 0.2$  sample measured at  $H = 6$  kOe.

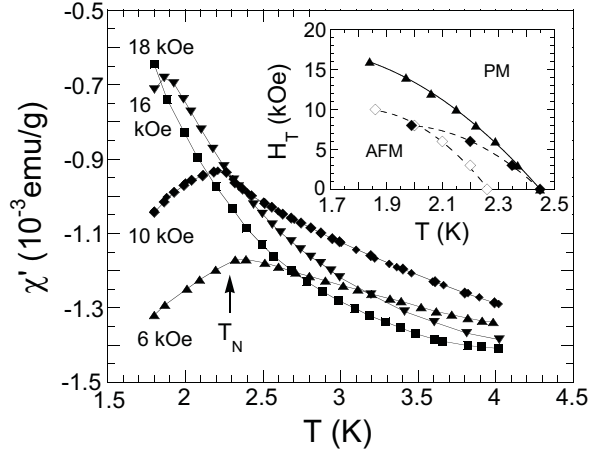


Fig. 7. Low temperature part of the ac susceptibility,  $\chi'$ , for the oxygen annealed  $\text{Gd}_{1+x}\text{Ba}_{2-x}\text{Cu}_3\text{O}_{7-\delta}$  sample with  $x = 0.2$  measured at several applied fields. The inset shows the  $H_T$ - $T$  phase diagram for the superconducting (triangles, solid line) and non-superconducting (diamonds, broken line) samples with  $x = 0.05$  (open symbols) and  $0.2$  (solid symbols).

annealed  $x = 0.2$  sample at several magnetic fields. Along with increasing  $H$ , the AFM peak shifts to lower temperatures, as expected. This observation is consistent with the results obtained for the specific heat measurements of the Gd123 non-substituted compound [50]. Results presented in Fig. 7 are used to construct the  $H_T$ - $T$  phase diagram, where  $H_T$  is a field for which the transition

from the AFM (or SF) to the PM phase occurs. Similar  $\chi_{ac}'(T)$  measurements have been performed for the non-superconducting  $x = 0.2$  sample annealed in Ar atmosphere. The  $H_T$ - $T$  phase diagram is shown in the inset of Fig. 7 for both the superconducting and the non-superconducting sample. A distinct difference between the  $H_T(T)$  dependencies is observed and this is important evidence that the superconducting  $x = 0.2$  sample is free of a significant amount of the oxygen deficient non-superconducting phase. In Fig. 7, the only single maximum is present for every  $\chi_{ac}'(T)$  curve, so we believe that the  $x = 0.2$  sample is homogenous and no separation of the magnetic superconducting and the magnetic normal phases appears. Thus, the  $\chi_{ac}'$  peak observed for the  $x = 0.2$  sample at  $T_N$  seems to be a result of the interaction between coexisting antiferromagnetic and superconducting subsystems.

## 4 Conclusion

Interaction between antiferromagnetism and superconductivity in low- $T_c$  materials is usually studied by measuring  $H_{c2}(T)$ ,  $H_{c1}(T)$ ,  $\chi_{ac}'(T)$ , and  $M(H)$  which reveal anomalies at  $T_N$  and  $H_{SF}$ . When the anomalous dependencies are known, the type of interaction between the long-range antiferromagnetic order and superconductivity may be determined. In this work, we examined the two-step flux penetration process for the initial magnetization of the classic magnetic superconductor DyMo<sub>6</sub>S<sub>8</sub>. This unusual flux penetration was interpreted as the consequence of the spin-flop phase appearing in the vortex core. Based on that observation and analyzing the free energy of a magnetic superconductor, the second penetration field for the two-step flux penetration, the superconducting coherence length, and the Ginzburg-Landau parameter were estimated. It was also shown that for the low- $T_c$  superconductor DyMo<sub>6</sub>S<sub>8</sub> the interaction between magnetic and conduction electrons is mostly electromagnetic. In the case of high- $T_c$  superconductors, some anomalies expected in the  $H_{c1}(T)$ ,  $M(H)$ , and  $\chi_{ac}'(T)$  dependencies were described for GdBa<sub>2</sub>Cu<sub>3</sub>O<sub>7- $\delta$</sub> , DyBa<sub>2</sub>Cu<sub>3</sub>O<sub>7- $\delta$</sub> , and Gd<sub>1+x</sub>Ba<sub>2-x</sub>Cu<sub>3</sub>O<sub>7- $\delta$</sub> , respectively. No unusual properties were found for those compounds except where Gd is partially substituted for Ba. For this compound, with  $x = 0.2$ , the interaction between antiferromagnetism and superconductivity leads to a peak in the  $T$  dependence of  $\chi_{ac}'$  at  $T_N$ . This observation was interpreted as a result of the pair-breaking effect that is present in a material where  $T_N$  is increased and  $T_c$  is decreased compared to the non-substituted compound. In non-substituted or weakly substituted Gd123 the interaction between magnetic and conduction electrons is very weak and the existing reorientation of the magnetic moments of the Gd ions at  $T_N$  is fully screened by superconductivity.

## Acknowledgements

The part concerning low- $T_c$  superconductors mainly emerged from work done with Drs. C. Sułkowski, E. Tjukanoff, and T. Krzyszton. The part about high- $T_c$  materials mainly based on work performed in close cooperation with Dr. Z. Bukowski, Prof. P. Esquinazi, and Prof. B. Dabrowski. The author also would like to acknowledge many stimulating discussions with T. Krzyszton and P. Tekiel. This work was supported by the State Committee for Scientific Research (KBN) within the Project No. 2 P03B 125 19.

## References

- [1] V.L. Ginzburg, Zh. Eksperim. Teor. Fiz. 31 (1956) 202 [Soviet Phys. JETP 4 (1957) 153].
- [2] A.A. Abrikosov and L.P. Gorkov, Zh. Eksperim. Teor. Fiz. 39 (1960) 1781 [Soviet Phys. JETP 12 (1961) 1243].
- [3] B.T. Matthias, H. Suhl and E. Corenzwit, Phys. Rev. Lett. 1 (1958) 92.
- [4] B.T. Matthias, H. Suhl and E. Corenzwit, Phys. Rev. Lett. 1 (1958) 449.
- [5] H. Suhl and B.T. Matthias, Phys. Rev. 114 (1959) 977, and references cited therein.
- [6] For a review, see M.B. Maple, Appl. Phys. 9 (1976) 179.
- [7] For a review, see M.B. Maple and Ø. Fischer (eds), Superconductivity in Ternary Compounds II, Topics in Current Physics, Vol. 34 (Springer-Verlag, 1982).
- [8] L.C. Gupta, J. Alloys and Comp. 262-263 (1997) 22.
- [9] For a review, see H. Schmidt and H.F. Braun, Studies in High Temperature Superconductors, Nova Science Publ., Inc., 26 (1998) 47.
- [10] For a review, see P.C. Canfield, P.L. Gammel and D.J. Bishop, Phys. Today, October (1998) 40-45.
- [11] For a review, see K.H. Muller and V.N. Narozhnyi, Rep. Prog. Phys. 64 (2001) 943-1008.
- [12] There is a considerable admixture of Y 4d as well as B 2p and C 2p electrons. See chapter 3 (Fig. 12) in Ref. [11] and references cited therein.
- [13] See chapter 4 in Ref. [11] and references cited therein.
- [14] M.B. Maple, J.M. Ferreira, R.R. Hake, B.W. Lee, J.J. Neumeier, C.L. Seaman, K.N. Yang and H. Zhou, J. Less-Common Metals 149 (1989) 405.

- [15] S.H. Liu, Phys. Rev. B 37 (1988) 7470.
- [16] T. Chattopadhyay, H. Maletta, W. Wirges, K. Fischer and P.J. Brown, Phys. Rev. B 38 (1988) 838.
- [17] For a review, see Ø. Fischer, Appl. Phys. 16 (1978) 1.
- [18] For a review, see H. Matsumoto and H. Umezawa, Cryogenics 1 (1983) 37.
- [19] For a review, see K.N. Shrivastava and K.P. Sinha, Phys. Reports, 115 (1984) 93.
- [20] H. Schmidt, M. Weber, H.F. Braun, Physica C 256 (1996) 393.
- [21] U. Welp, W.K. Kwok, G.W. Crabtree, K.G. Vandervoort and J.Z. Liu, Phys. Rev. Lett. 62 (1989) 1908.
- [22] K. Nakao, N. Miura, K. Tatsuhara, S. Uchida, H. Takagi, T. Wada and S. Tanaka, Nature 332 (1988) 816.
- [23] K. Rogacki, C. Sułkowski, A.J. Zaleski, Z. Bukowski, B. Greń, R. Horyń, E. Trojnar and J. Klamut, phys. stat. sol. (b) 146 (1988) K103.
- [24] K. Rogacki and C. Sułkowski, Physica C, 153-155 (1988) 483.
- [25] T. Krzyszton, J. Mag. Mater. 15-17 (1980) 1572.
- [26] T. Krzyszton, Phys. Lett. 104A (1984) 225.
- [27] K. Rogacki, E. Tjukanoff and S. Jaakkola, Phys. Rev. B 64 (2001) 094520.
- [28] T. Krzyszton and K. Rogacki, Europ. J. Phys. B (2002) 181.
- [29] M. Tachiki, H. Matsumoto and H. Umezawa, Phys. Rev. B 20 (1979) 1915.
- [30] H. Matsumoto, R. Teshima, H. Umezawa and M. Tachiki, Phys. Rev. B 27 (1983) 158.
- [31] K.E. Gray, J. Zasadzinski, R. Vaglio and D. Hinks, Phys. Rev. B 27 (1983) 4161.
- [32] K. Rogacki and C. Sułkowski, Modern Phys. Lett. 6 (1992) 41.
- [33] T. Krzyszton, Phys. Lett. A 190 (1994) 196.
- [34] T. Krzyszton, Physica C 340 (2000) 156.
- [35] K. Rogacki, P. Esquinazi, E. Faulhaber and W. Sadowski, Physica C 246 (1995) 123.
- [36] P. Fischer, K. Kakurai, M. Steiner, K.N. Clausen, B. Lebech, F. Hulliger, H.R. Ott, P. Brüesch and P. Unternährer, Physica C 152 (1988) 145.
- [37] T.W. Clinton, J.W. Lynn, J.Z. Liu, Y.X. Jia and R.N. Shelton, J. Appl. Phys. 70 (1991) 5751.

- [38] J.D. Jorgensen, B.W. Veal, A.P. Paulikas, L.J. Nowicki, G.W. Crabtree, H. Claus and W.K. Kwok, *Phys. Rev. B* 41 (1990) 1863.
- [39] T. Graf, G. Triscone and J. Muller, *J. Less-Common Metals* 159 (1990) 349.
- [40] T. Krekels, H. Zou, G. Van Tendeloo, D. Wagener, M. Buchgeister, S.M. Hosseini and P. Herzog, *Physica C* 196 (1992) 363.
- [41] S. Li, E.A. Hayri, K.V. Ramanujachary and M. Greenblatt, *Phys. rev. B* 38 (1988) 2450.
- [42] T. Wada, N. Suzuki, A. Maeda, T. Yabe, K. Uchinokura, S. Uchida and S. Tanaka, *Phys. Rev. B* 39 (1989) 9126.
- [43] R.A.M. van Woerden and D.M. de Leeuw, *Physica C* 165 (1990) 221.
- [44] K. Takita, H. Akinaga, T. Ohshima, Y. Takeda and M. Takano, *Physica C* 191 (1992) 509.
- [45] B.W. Veal, W.K. Kwok, A. Umezawa, G.W. Crabtree, J.D. Jorgensen, J.W. Downey, L.J. Nowicki, A.W. Mitchell, A.P. Paulikas and C.H. Sowers, *Appl. Phys. Lett.* 51 (1989) 279.
- [46] B. Dabrowski, K. Rogacki, J.W. Koenitzer, K.R. Poeppelmeier and J.D. Jorgensen, *Physica C* 277 (1997) 24.
- [47] K. Rogacki, B. Dabrowski, O. Chmaissem and J.D. Jorgensen, *Phys. Rev. B* 63 (2000) 054501.
- [48] K.M. Beauchamp, G.C. Spalding, W.H. Huber and A.M. Goldman, *Phys. Rev. Lett.* 73 (1994) 2752.
- [49] T. Plackowski, C. Sułkowski, Z. Bukowski, D. Włosewicz and K. Rogacki, *Physica C* 254 (1995) 331.
- [50] H.P. van der Meulen, J.J.M. Franse, Z. Tarnawski, K. Kadowaki, J.C.P. Klaasse and A.A. Menovsky, *Physica C* 152 (1988) 65.